Investigation of the quantum cantori regime in quarter-stadium billiards

Nazar Savytskyy and Leszek Sirko
Institute of Physics, Polish Academy of Sciences, Aleja Lotników 32/46, 02-668 Warszawa, Poland
(Received 25 February 2002; published 10 June 2002)

We study experimentally and numerically the regime of quantum cantori in quarter-stadium billiards. Experimentally, a quarter-stadium billiard is simulated by a thin quarter-stadium microwave cavity. Using a field perturbation technique and a circular wave expansion method we reconstruct the eigenfunctions of the quarter-stadium microwave billiard with the parameter $\varepsilon=0.1$ in the cantori regime $N=7-63$. The quarter-stadium billiards with $\varepsilon=0.1$ and 0.05, respectively, are also investigated numerically. We show that in the quantum cantori regime the rescaled localization length of the eigenfunctions fluctuates around a value that depends on the parameter ε.

DOI: 10.1103/PhysRevE.65.066202 PACS number(s): 05.45.Mt

The Kolmogorov-Arnold-Moser (KAM) theorem [1] allows us to understand that classical chaos may be confined to certain regions of phase space. KAM tori can act as impenetrable barriers to the probability flow. With increasing nonlinearity of the system the KAM tori break up into cantori [2,3] and become partially penetrable to the chaotic orbits. Amazingly, in quantum mechanics classical cantori appear to act as dynamical barriers that can entirely inhibit the diffusive growth [4]. Recently, theoretical analysis of classical and quantum properties of stadium billiards has led to the identification of four different localized regimes, namely, perturbative, cantori, dynamical, and ergodic [5,6,8]. The dynamical localization regime and the ergodic regime exist also in rough billiards and were the subject of intensive theoretical [9–11] and experimental [12,13] work. Casati and Prosen [6,7] have shown for the quarter-stadium billiards that in the quantum cantori regime (approximately given by $\frac{1}{16}\varepsilon^{-2}<N<\frac{1}{16}\varepsilon^{-3}$) the rescaled localization length of the eigenfunctions is constant. In this paper we put this theoretical finding into experimental and numerical tests.

Experimentally, eigenfunctions (electric field) were evaluated for the thin (height $h=8$ mm) microwave cavity with the shape presented in Fig. 1. The microwave cavity simulates the quarter-stadium billiard with the parameter $\varepsilon=a/R=0.1$ due to the equivalence between the Schrödinger equation and the Helmholtz equation. This equivalence remains valid for frequencies less than the cutoff frequency $\nu_c=c/2h\simeq 18.7$ GHz, where c is the speed of light.

We show that eigenfunctions $\Psi_N(r,\theta)$ [electric field distribution $E_N(r,\theta)$ inside the cavity, N is the level number] can be determined from the form of $E_N(R_c,\theta)$ evaluated on a quarter circle of fixed radius R_c (see Fig. 1). The first step in evaluation of $E_N(R_c,\theta)$ is measurement of $E_N(R_c,\theta)^2$. The perturbation technique developed in Ref. [14] and used successfully in Refs. [14–17] was implemented for this purpose. In this method a small perturber is introduced inside the cavity to alter its resonant frequency according to

$$\nu-\nu_N=\nu_N(aB_N^2-bE_N^2), \tag{1}$$

where ν_N is the Nth resonant frequency of the unperturbed cavity, a and b are geometrical factors. Equation (1) shows that the formula cannot be used to evaluate E_N^2 until the term containing magnetic field B_N vanishes. To minimize the influence of B_N on the frequency shift $\nu-\nu_N$ a dielectric perturber [18] containing a small piece of a metallic pin was used. The perturber was a dielectric sphere of 3.0 mm diameter. A small piece of a metallic pin was introduced inside the perturber in order to move it with a magnet placed on the top of the cavity. The size of the pin (2.0 mm in length and 0.40 mm in diameter) was chosen to be the smallest possible that still allowed the perturber to follow smoothly the magnet during its movement. Relatively weak interaction between the magnet and the perturber minimized the friction between the sphere and the wall and improved the accuracy of positioning of the perturber inside the cavity. For the same purpose additional lubrication of the cavity's wall was used. Using such a perturber we had no positive frequency shifts that would exceed the uncertainty of frequency shift measurements (20 kHz). The resonant frequency variation connected with the thermal expansion of the brass cavity was estimated to be 180 kHz/deg at $\nu_{63}\simeq 7.6$ GHz and was not negligible in comparison to the typical frequency shift of 1

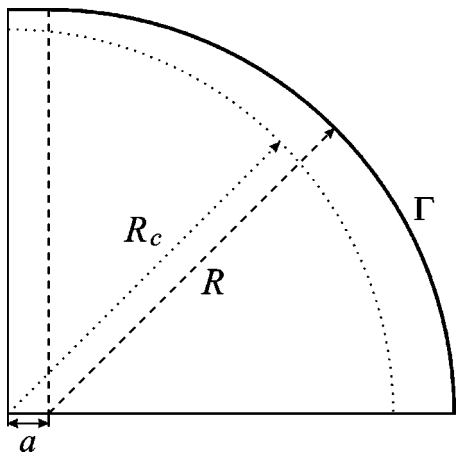

FIG. 1. The quarter-stadium billiard with radius R and straight segment a. In the experiment the quarter-stadium microwave billiard with $R=20$ cm and $a=2$ cm (parameter $\varepsilon=a/R=0.1$) was used. Squared eigenfunctions $|\Psi_N(R_c,\theta)|^2$ (see text) were evaluated on a quarter circle of fixed radius $R_c=19$ cm. The billiard's boundary Γ is marked with the bold line.

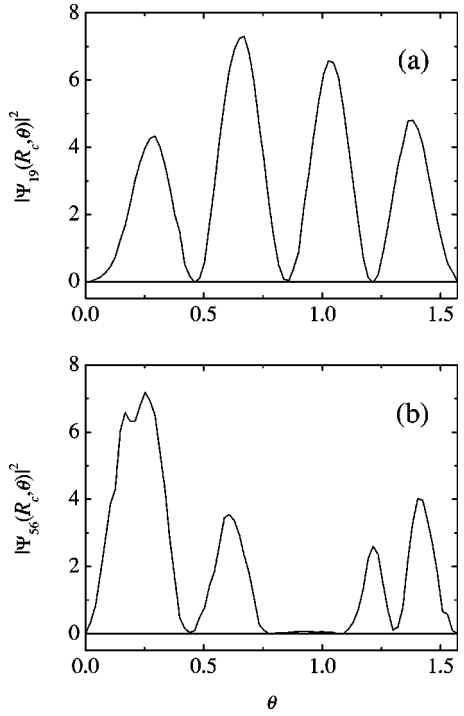

FIG. 2. Squared eigenfunctions $|\Psi_N(R_c,\theta)|^2$ (in arbitrary units) measured on a quarter circle with radius $R_c=19$ cm (see Fig. 1) with the level numbers: (a) $N=19$ ($\nu_{19}\simeq 4.37$ GHz), (b) $N=56$ ($\nu_{56}\simeq 7.17$ GHz).

MHz caused by the perturber. To eliminate this effect the temperature of the cavity was stabilized with the accuracy of 0.05°.

The regime of quantum cantori for the experimental quarter-stadium billiard ($\varepsilon=0.1$) is defined for $N=7$–63. Using a field perturbation technique we measured squared eigenfunctions $|\Psi_N(R_c,\theta)|^2$ for 36 modes within the specified region. The range of corresponding eigenfrequencies was from $\nu_7=3.04$ GHz to $\nu_{63}=7.59$ GHz. The measurements were performed at 2 mm steps along a quarter circle with fixed radius $R_c=19$ cm. This step was small enough to reveal in details the space structure of low-lying levels. In Fig. 2 we show the examples of the squared eigenfunction $|\Psi_N(R_c,\theta)|^2$ evaluated for levels 19 and 56. The perturbation method used in our measurements allows us to extract information about the eigenfunction amplitude $|\Psi_N(R_c,\theta)|$ at any given point of the cavity but it does not allow to determine the sign of $\Psi_N(R_c,\theta)$ [19]. Numerical calculations performed for the quarter-stadium billiards (e.g., Ref. [20]) suggest the following sign-assignment strategy. We begin with the identification of all close to zero minima of $|\Psi_N(R_c,\theta)|$. Then the sign ''minus'' maybe arbitrarily assigned to the region between the first and the second minimum, ''plus'' to the region between the second minimum and the third one, the next ''minus'' to the next region between consecutive minima and so on. In this way we construct our ''trial eigenfunction'' $\Psi_N(R_c,\theta)$. If the assignment of the signs is correct we should reconstruct the eigenfunction $\Psi_N(r,\theta)$ inside the billiard with the boundary condition $\Psi_N(r_\Gamma,\theta_\Gamma)=0$.

As was proposed in Ref. [6], eigenfunctions of a quarter-stadium billiard may be expanded in terms of circular waves (here only odd-odd states in expansion are considered)

$$\Psi_N(r,\theta)=\sum_{s=1}^{M} a_s C_s J_{2s}(k_N r)\sin(2s\theta), \tag{2}$$

where

$$C_s=[(\pi/4)\textstyle\int_0^{r_{max}}|J_{2s}(k_N r)|^2 r\,dr]^{-1/2}$$

and

$$k_N=2\pi\nu_N/c$$

.

In Eq. (2) the number of basis functions is limited to $M=k_N r_{max}/2=l_N^{max}/2$, with $r_{max}=R+a$. $l_N^{max}=k_N r_{max}$ is a semiclassical estimate for the maximum possible angular momentum for a given k_N. Circular waves with angular momentum $2s>2M$ correspond to evanescent waves and can be neglected. Coefficients a_s may be extracted from the ''trial eigenfunction'' $\Psi_N(R_c,\theta)$ via

$$a_s=\left[\frac{\pi}{4}C_s J_{2s}(k_N R_c)\right]^{-1}\int_0^{\pi/2}\Psi_N(R_c,\theta)\sin(2s\theta)\,d\theta. \tag{3}$$

Since our ''trial eigenfunction'' $\Psi_N(R_c,\theta)$ is only defined on a quarter circle of fixed radius R_c and is not normalized we imposed normalization of the coefficients a_s, $\Sigma_{s=1}^{M}|a_s|^2=1$. Now, the coefficients a_s and Eq. (2) can be used to reconstruct the eigenfunction $\Psi_N(r,\theta)$ of the billiard. Figures 3 and 4 show reconstructed eigenfunction $\Psi_{19}(r,\theta)$ of the billiard for two different sign assignments in the ''trial eigenfunction'' $\Psi_{19}(R_c,\theta)$. Due to experimental uncertainties and the finite step size in the measurements of $|\Psi_N(R_c,\theta)|^2$ the eigenfunctions $\Psi_N(r,\theta)$ are not exactly zero at the boundary Γ. As the quantitative measure of the sign assignment quality we chose the integral $\int_\Gamma|\Psi_N(r,\theta)|dl$ calculated along the billiard's boundary Γ. For the two cases in Figs. 3 and 4 we got the values of 0.086 and 1.281, respectively, which clearly show that the reconstruction of the eigenfunction $\Psi_{19}(r,\theta)$ was done properly only in the first case (Fig. 3). Using the method of the ''trial eigenfunction'' we were able to reconstruct 36 experimental eigenfunctions of the quarter-stadium billiard with the level number N between 7 and 63. The remaining 21 eigefunctions from the quantum cantori region $N=7$–63 were not reconstructed due to the problems with the measurements of $|\Psi_N(R_c,\theta)|^2$ along a quarter circle coinciding with one of the nodal lines of $\Psi_N(r,\theta)$.

The localization length ℓ of the experimental eigenfunctions $\Psi_N(r,\theta)$ was estimated using the following formula:

$$\ell=\beta\min\left\{\mathcal{N}_A;\sum_{s\in A}|a_s|^2\geqslant 0.99\right\}, \tag{4}$$

where the numerical constant $\beta=2\times 1.38$ [6]. The 99% localization length (4) is proportional to the minimal number

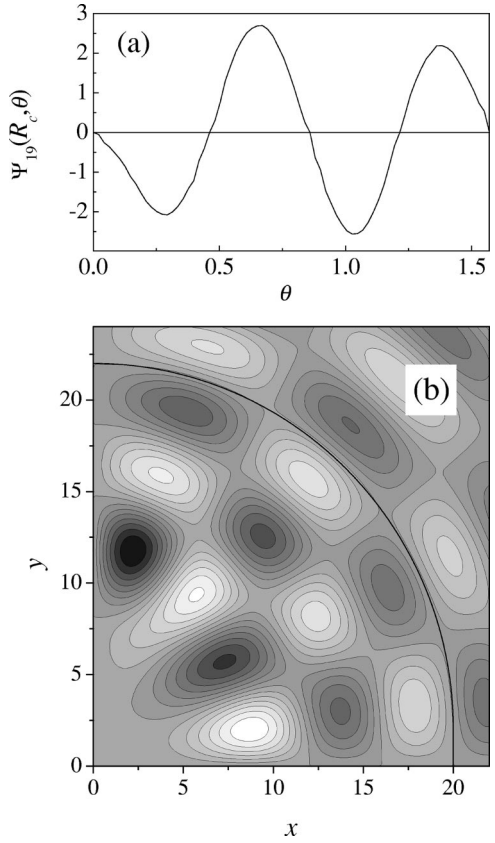

FIG. 3. Panel (a), ''trial eigenfunction'' $\Psi_{19}(R_c,\theta)$ obtained from the measured $|\Psi_{19}(R_c,\theta)|^2$ using a sign assignment strategy $(-,+,-,+,\ldots)$. Panel (b), eigenfunction of the experimental billiard $\Psi_{19}(r,\theta)$ reconstructed from the ''trial eigenfunction'' $\Psi_{19}(R_c,\theta)$. The amplitudes have been converted into a gray scale with white corresponding to large positive and black corresponding to large negative values, respectively. Dimensions of the billiard are given in centimeters. Let us note that the eigenfunction $\Psi_{19}(r,\theta)$ has proper boundary conditions, $\Psi_{19}(r_\Gamma,\theta_\Gamma)\simeq 0$ (see text).

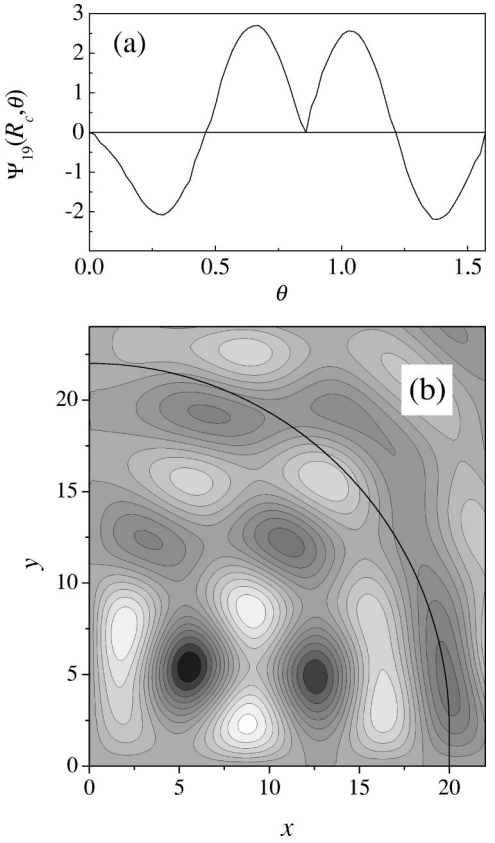

FIG. 4. Panel (a), another ''trial eigenfunction'' $\Psi_{19}(R_c,\theta)$ obtained from the measured $|\Psi_{19}(R_c,\theta)|^2$. Panel (b) eigenfunction $\Psi_{19}(r,\theta)$ reconstructed from the ''trial eigenfunction'' $\Psi_{19}(R_c,\theta)$ does not fulfill the boundary conditions $\Psi_{19}(r_\Gamma,\theta_\Gamma)\simeq 0$ and has to be rejected. The amplitudes have been converted into a gray scale with white corresponding to large positive and black corresponding to large negative values, respectively. Dimensions of the billiard are given in centimeters.

$\mathcal{N}_A$ of circular eigenfunctions that are needed to support 99% probability. Such a choice of the localization length is connected with the fact that for the stadium billiard localization is algebraic [6]. Casati and Prosen [6] observed that the 99% localization length is the least sensitive to the slowly decaying tails of the distribution $|a_s|^2$.

In Fig. 5 we show the rescaled localization length $\sigma = \ell / l_N^{max}$ calculated for the experimental eigenfunctions $\Psi_N(r,\theta)$ lying in the quantum cantori region $N=7$–63 versus the scaling variable $x=\varepsilon^{3/2}k_N R$. Each point is obtained by averaging over five eigenstates. The least-squares fit to the experimental data gave the line whose slope 0.05 ± 0.11 agrees within the error with the expected slope of 0. The average value of the rescaled localization length $\overline{\sigma}$ was estimated to be 0.72 ± 0.02. Figure 5 provides the experimental confirmation of the predicted existence of the quantum cantori regime where the rescaled localization length of the eigenfunctions does not depend on average on the level number N.

Investigation of the quantum cantori regime for billiards with smaller parameter ε requires estimation of eigenfunctions with much higher level numbers, e.g., $25<N<500$ for $\varepsilon=0.05$. Due to experimental limitations [e.g., step of 2 mm in measurements of $|\Psi_N(R_c,\theta)|^2$] we could not do it experimentally. Instead we decided to analyze such a billiard numerically. Eigenfunctions of the quarter-stadium billiard ($R=20$ cm, $a=1$ cm, and $\varepsilon=a/R=0.05$) were calculated using the method based on the Green's function approach, BIM (the boundary integral method) [21,11]. This method was also used to calculate eigenfunctions ($N=7$–63) for our experimental quarter-stadium billiard. It was tested [11] that BIM allows for effective calculation of relatively low eigenvalues and eigenfunctions of quantum billiards ($N<1000$) and from this point of view it can be treated as complementary to the method of Vergini and Saraceno [22] used in Ref. [6] that works very efficiently for much higher N.

In Fig. 5 we show our numerical results. For $\varepsilon=0.1$ the rescaled localization length σ is compared to the experimental one. As we see, the agreement is very good. Also here each point is obtained by averaging over five eigenstates. For the billiard with the parameter $\varepsilon=0.05$ the rescaled localization length σ also does not depend on the scaling variable x. Each point in these calculations is obtained by averaging

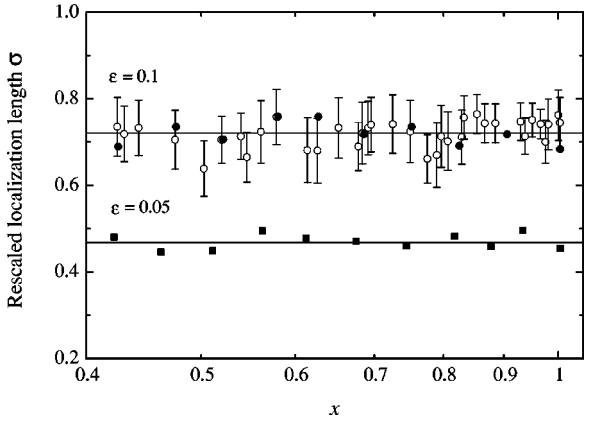

FIG. 5. Rescaled localization length $\sigma = \ell / l_N^{max}$ versus the scaling variable $x = \varepsilon^{3/2} k_N R$ in the regime of quantum cantori. For the quarter-stadium billiard with $\varepsilon = 0.1$ experimental results (empty circles) are compared with the numerical ones (full circles). In both cases points were obtained by averaging over five eigenstates. The solid line marks the average value of experimental rescaled localization length $\overline{\sigma} = 0.72 \pm 0.02$. For the billiard with $\varepsilon = 0.05$ numerical results (full squares) are presented. Each point was obtained by averaging over 25 consecutive eigenstates. The solid line shows the average value $\overline{\sigma} = 0.47 \pm 0.01$ obtained by averaging over all 424 numerically calculated eigenstates ($N = 76$–499).

over 25 consecutive eigenstates. Such a behavior of the rescaled localization length σ strongly supports the existence of the quantum cantori regime in quarter-stadium billiards. The average value of the rescaled localization length $\overline{\sigma} \simeq 0.47 \pm 0.01$ is smaller than the one obtained for the billiard with $\varepsilon = 0.1$. Moreover, according to formulas (7) and (17) in Ref. [6], $\overline{\sigma} = \overline{p} = \kappa\varepsilon$, where $\overline{p}$ is the average size of classical cantori and κ is some numerical constant, the average size of classical cantori for the billiard with $\varepsilon = 0.05$ is smaller than for the billiard with $\varepsilon = 0.1$.

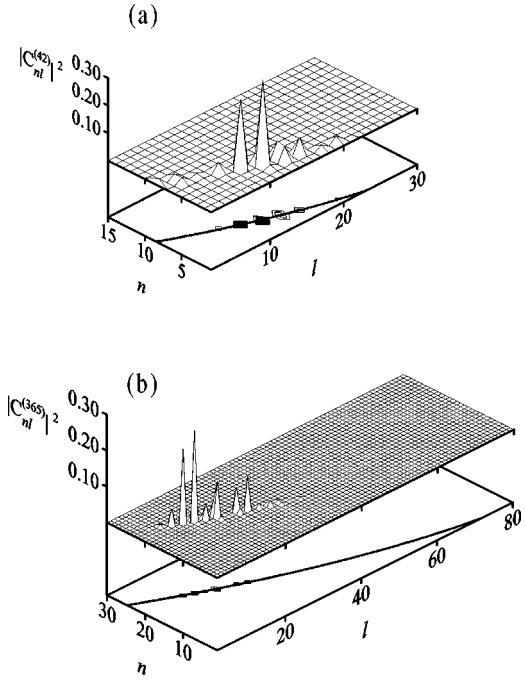

FIG. 6. Structure of the energy surface in the regime of quantum cantori. Here we show the squared amplitudes $|C_{nl}^{(N)}|^2$ for the eigenfunctions: (a) $N = 42$ ($\varepsilon = 0.1$), (b) $N = 365$ ($\varepsilon = 0.05$). In both cases the eigenfunctions are localized in the n,l basis. Solid lines show the semiclassical estimation of the energy surface (see text).

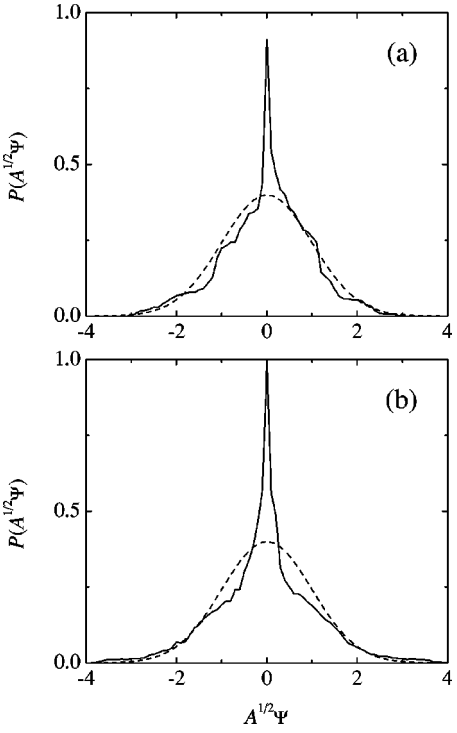

FIG. 7. Amplitude distribution $P(\Psi A^{1/2})$ for the eigenstates. (a) $N = 42$ ($\varepsilon = 0.1$) and (b) $N = 365$ ($\varepsilon = 0.05$) constructed as histograms with bin equal to 0.1. The width of the distribution $P(\Psi)$ was rescaled to unity by multiplying normalized to unity eigenfunction by the factor $A^{1/2}$, where A denotes the billiard's area. The dashed line shows the standard normalized Gaussian prediction $P_0(\Psi A^{1/2}) = (1/\sqrt{2\pi}) e^{-\Psi^2 A/2}$.

Knowledge of the billiard's eigenfunctions allows us to find the structure of the energy surface in the regime of quantum cantori. For this reason we extracted eigenfunction amplitudes $C_{nl}^{(N)} = \langle n,l|N\rangle$ in the basis n,l of a quarter-circular billiard with radius r_{max}, where $n = 1,2,3,\ldots$ enumerates the zeros of the Bessel functions and $l = 1,2,3,\ldots$ is the angular quantum number. The squared amplitudes $|C_{nl}^{(N)}|^2$ and their projections into the energy surface for the representative experimental eigenfunction ($N = 42$, $\varepsilon = 0.1$) and the numerical eigenfunction ($N = 365$, $\varepsilon = 0.05$) are shown in Figs. 6(a) and 6(b), respectively. In both cases the eigenfunctions are localized in the n,l basis. The full lines on the projection planes in Fig. 6 mark the energy surface of a quarter-circular billiard $H(n,l) = E_N = k_N^2$ estimated from the semiclassical formula [13]: $\sqrt{(l_N^{max})^2 - l^2} - l \arctan[l^{-1}\sqrt{(l_N^{max})^2 - l^2}] + \pi/4 = \pi n$. The peaks $|C_{nl}^{(N)}|^2$ are spread almost perfectly along the line marking the energy surface. It is worth noting that in the regime of Shnirelman ergodicity investigated in rough billiards [11] the eigenstates are extended over the whole energy surface.

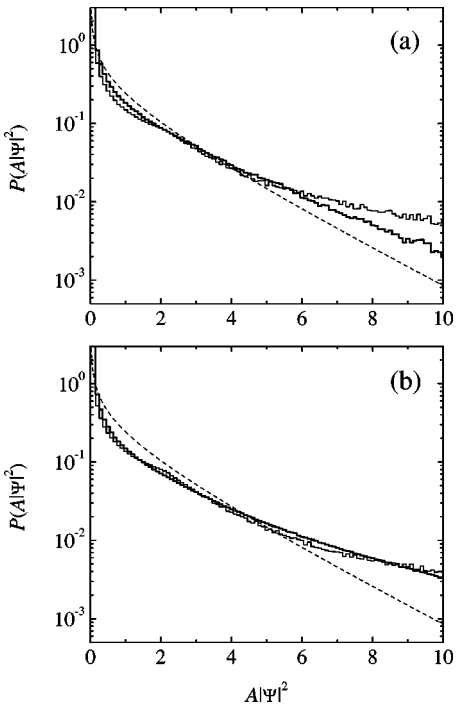

FIG. 8. The spatial intensity distribution $P(A|\Psi|^2)$ of the measured and calculated eigenfunctions. Panel (a), the bold line shows $P(A|\Psi|^2)$ calculated for 36 experimental eigenfunctions (range of $N=7-63$) of the quarter-stadium billiard with $\varepsilon=0.1$ compared to the Thomas-Porter distribution (dashed line) and the intensity distribution $P(A|\Psi|^2)$ evaluated for a quarter-circular billiard with radius $R=22$ cm (thin line). In calculations of $P(A|\Psi|^2)$ for a quarter-circular billiard only eigenstates with the level number $N=7-63$ were taken into account. Panel (b), the bold line shows $P(A|\Psi|^2)$ calculated for 424 numerical eigenfunctions ($N=76-499$) of the quarter-stadium billiard with $\varepsilon=0.05$ compared to the Thomas-Porter distribution (dashed line) and the intensity distribution $P(A|\Psi|^2)$ evaluated for a quarter-circular billiard with radius $R=22$ cm (thin line). $P(A|\Psi|^2)$ for a quarter-circular billiard was calculated for eigenstates with the level numbers $N=76-499$.

An additional confirmation of nonergodic behavior of the measured and calculated eigenfunctions can be also sought in the form of the amplitude distribution $P(\Psi)$ [23,20]. For irregular, chaotic states the probability of finding the value Ψ at any point inside the billiard, without knowledge of the surrounding values, should be distributed as a Gaussian, $P(\Psi)\sim e^{-\beta\Psi^2}$. The amplitude distributions $P(\Psi A^{1/2})$ for the experimental eigenfunction $N=42$ ($\varepsilon=0.1$) and the numerical one $N=365$ ($\varepsilon=0.05$) are shown in Fig. 7. They were constructed as normalized to unity histograms with the bin equal to 0.1. Each particular histogram was built using approximately 48 000 values of an eigenfunction. The width of the amplitude distribution $P(\Psi)$ was rescaled to unity by multiplying normalized to unity eigenfunction by the factor $A^{1/2}$, where A denotes billiard's area (see formula (23) in Ref. [20]). For all measured and calculated eigenfunctions (results presented in Fig. 7 are no exceptions) there is no agreement with the standard normalized Gaussian prediction $P_0(\Psi A^{1/2})=(1/\sqrt{2\pi})e^{-\Psi^2 A/2}$ that strongly suggests that chaos is suppressed in the quantum cantori regime.

Finally, we calculated the spatial intensity distribution $P(A|\Psi|^2)$ of the measured and calculated eigenfunctions. Our results are presented in Fig. 8. In the calculations of $P(A|\Psi|^2)$, 36 experimental eigenfuctions in the range of $N=7-63$ [Fig. 8(a)] and 424 numerical eigenfuctions $N=76-499$ [Fig. 8(b)] were included. The deviation from the Porter-Thomas distribution predicted for chaotic systems is very significant. For comparison, we also show the intensity distribution $P(A|\Psi|^2)$ evaluated for a quarter-circular billiard with radius $R=22$ cm. It is interesting to note that the intensity distributions calculated in the regime of quantum cantori are much closer to the distributions calculated for a quarter-circular billiard than to the Porter-Thomas distribution.

In summary, we evaluated experimentally and numerically eigenfunctions for quarter-stadium billiards in the regime of quantum cantori. We showed that in the quantum cantori regime the rescaled localization length of the eigenfunctions fluctuates around a value that depends on the parameter ε. We demonstrated that in the regime of quantum cantori the eigenfunctions are localized in the n,l basis, the amplitude distributions $P(\Psi A^{1/2})$ are different from the standard normalized Gaussian prediction $P_0(\Psi A^{1/2})=(1/\sqrt{2\pi})e^{-\Psi^2 A/2}$, and the spatial intensity distributions $P(A|\Psi|^2)$ of the measured and calculated eigenfunctions deviate from the Porter-Thomas distribution.

N.S. and L.S. acknowledge partial support by KBN Grant No. 2 P03B 023 17. We thank G. Casati, Sz. Bauch, and T. Prosen for stimulating discussions.

[1] V. I. Arnold, *Mathematical Methods of Classical Mechanics* (Springer-Verlag, New York, 1989).
[2] R.S. MacKay, J.D. Meiss, and I.C. Persival, Physica **13D**, 55 (1984).
[3] D. Bensimov and L.P. Kadanoff, Physica **13D**, 82 (1984).
[4] T. Geisel, G. Radons, and J. Rubner, Phys. Rev. Lett. **57**, 2883 (1986).
[5] F. Borgonovi, G. Casati, and B. Li, Phys. Rev. Lett. **77**, 4744 (1996).
[6] G. Casati and T. Prosen, Physica D **131**, 293 (1999).
[7] G. Casati and T. Prosen, Phys. Rev. E **59**, R2516 (1999).
[8] F. Borgonovi, P. Conti, D. Rebuzzi, B. Hu, and B. Li, Physica D **131**, 317 (1999).
[9] K. Frahm and D. Shepelyansky, Phys. Rev. Lett. **78**, 1440 (1997).
[10] K. Frahm and D. Shepelyansky, Phys. Rev. Lett. **79**, 1833 (1997).
[11] Y. Hlushchuk, A. Bl̨edowski, N. Savytskyy, and L. Sirko, Phys. Scr. **64**, 192 (2001).
[12] L. Sirko, Sz. Bauch, Y. Hlushchuk, P.M. Koch, R. Blümel, M. Barth, U. Kuhl, and H.-J. Stöckmann, Phys. Lett. A **266**, 331 (2000).

[13] Y. Hlushchuk, L. Sirko, U. Kuhl, M. Barth, and H.-J. Stöckmann, Phys. Rev. E **63**, 046208 (2001).
[14] L.C. Maier and J.C. Slater, J. Appl. Phys. **23**, 68 (1952).
[15] S. Sridhar, Phys. Rev. Lett. **67**, 785 (1991).
[16] C. Dembowski, H.-D. Gräf, A. Heine, R. Hofferbert, H. Rehfeld, and A. Richter, Phys. Rev. Lett. **84**, 867 (2000).
[17] D.H. Wu, J.S.A. Bridgewater, A. Gokirmak, and S.M. Anlage, Phys. Rev. Lett. **81**, 2890 (1998).
[18] P.M. Koch, Physica D **83**, 178 (1995).
[19] J. Stein, H.-J. Stöckmann, and U. Stoffregen, Phys. Rev. Lett. **75**, 53 (1995).
[20] S.W. McDonald and A.N. Kaufman, Phys. Rev. A **37**, 3067 (1988).
[21] I. Kosztin and K. Schulten, Int. J. Mod. Phys. C **8**, 293 (1997).
[22] E. Vergini and M. Saraceno, Phys. Rev. E **52**, 2204 (1995).
[23] M.V. Berry, J. Phys. A **10**, 2083 (1977).